IEEE Access
Multidisciplinary | Rapid Review | Open Access Journal

Received July 2, 2018, accepted August 9, 2018, date of publication August 17, 2018, date of current version September 7, 2018.

Digital Object Identifier 10.1109/ACCESS.2018.2865929

Investigation of Terahertz 3D EM Simulation on Device Modeling and A New InP HBT Dispersive Inter-Electrode Impedance Extraction Method

YAPEI CHEN[1], YONG ZHANG[1], (Senior Member, IEEE), YUEHANG XU[1], (Senior Member, IEEE), YAN SUN[2], WEI CHENG[2], HAIYAN LU[2], FEI XIAO[1], AND RUIMIN XU[1], (Member, IEEE)

[1]EHF Key Laboratory of Fundamental Science, University of Electronic Science and Technology of China, Chengdu 611731, China
[2]Science and Technology on Monolithic Integrated Circuits and Modules Laboratory, Nanjing Electronic Devices Institute, Nanjing 210016, China

Corresponding author: Yong Zhang (yongzhang@uestc.edu.cn)

ABSTRACT In this paper, a new 3-D electromagnetic (EM) simulation approach for heterojunction bipolar transistor (HBT) parameter extraction in terahertz band is presented. We introduce an inter-electrode impedance equivalent-circuit model with the concept of dispersive parameters and a more rigorous 3-D EM simulation parameter extraction method to avoid serious discrepancies between the simulated EM field distribution and the real EM field distribution of the device. Terahertz parasitic effects, including the EM field discretization and multi-finger device field sharing, are observed. Compared with the previous 3-D EM simulation-assisted model, the new model in this paper demonstrates better results for multi-finger indium phosphide HBTs.

INDEX TERMS InP HBT, terahertz band, 3D EM simulation, transistor model.

I. INTRODUCTION

Indium phosphide (InP) based heterojunction bipolar transistor (HBT) and high electron mobility transistor (HEMT) have been demonstrated with output maximum frequency of oscillation exceeding one terahertz (THz) [1]–[3], and they have been applied in various circuits and systems in terahertz band [3]. Up to now, many high-frequency device models have been reported [4]–[8].

Parasitic effects influence the device frequency performance seriously. Their impact is even comparable with the active device in terahertz band, which should be modeled carefully. Three-dimension (3D) electromagnetic (EM) simulation makes it possible to investigate parasitic effects in complex devices and circuits. 3D EM simulation has been implemented on on-wafer parasitic parameter de-embedding and peripheral passive element extraction [9]–[11]. As for the high-frequency device modeling, researchers also apply 3D EM simulation on the whole device to promote the development of high-frequency models [4]–[8].

Generally, an analytical or a direct inter-electrode parameter extraction method is a better choice than a fitting method. However, there are problems in direct extraction methods incorporated with 3D EM simulation at high frequencies. For example, many direct parasitics extraction methods are not based on the EM field distribution of the whole device structure, but usually processed by step-by-step parameter peeling and simplification of the device [4]–[8]. As for the low frequency equivalent circuit modeling, equivalent circuits can be simplified under different DC biases. Then, with a mathematical derivation, extrinsic elements can be calculated directly with methods in [12]–[14]. However, as for the high-frequency device 3D modeling, the core of an accurate 3D model is the overall EM field distribution, so 3D device models are not easy to be simplified like equivalent circuits. Another problem is that in some multi-step extraction processes with 3D EM simulation, there are too many simplified 3D sub-circuits [5], [6]. Parasitic elements in 3D EM simulation are relevant to the device field distribution (field-distribution-relevant), however, some of the omitted or repeated structures in 3D sub-circuit models actually make the EM field uncontrollable, which could result in unreliable parameters. These methods can be used to extract parasitic parameters of simple structure devices in THz band to some degree, but are with pitfalls when

applied to multi-finger or complex structure devices. More rigorous 3D EM simulation parameter extraction method is required for THz complex structure device modeling.

The inter-electrode impedance model in this work is called dispersive for the reason that their value is closely related to the EM field distribution in the device. Therefore, they are frequency relevant. There could be a question why parasitic elements in low-frequency devices are constant, as they are also obviously related to the EM field distribution. It is because that the wavelength is much longer than the device length at low frequencies. No matter how the frequency changes, the EM field distribution is the same. However, THz devices sometimes work at real high frequencies, or a very broad frequency range has to be considered. The EM field distribution will show difference, and different EM field distribution conditions impact the inter-electrode impedance which is important in high-frequency device modeling.

In Section II, a discussion about the multi-step 3D EM parameter extraction method of a single-finger HBT is presented. We point out the field distortion problem in some improper simplified 3D simulation structures. In Section III and IV, we propose an applicable dispersive inter-electrode impedance extraction method with a more strict overall 3D EM simulation procedure. A modified inter-electrode impedance model and assistance 3D EM simulation structures are presented in Section III. The inter-electrode impedance of a two-finger InP HBT is extracted in a broad frequency range in Section IV. In Section V, the proposed inter-electrode impedance model and a conventional small-signal internal device model are combined together. The new method is then verified by comparisons between measured and simulated S-parameters with different 3D EM simulation assisted models. Finally, conclusion is given in section VI.

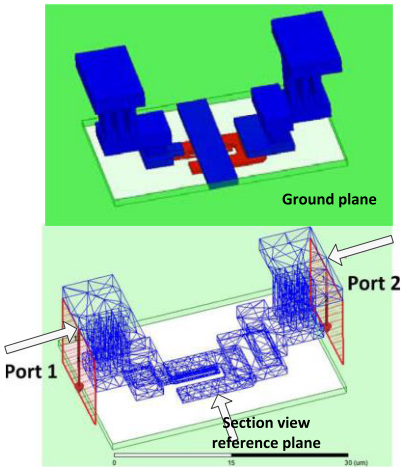

FIGURE 1. 3D model and port setting of a single-finger HBT redrawn from [6].

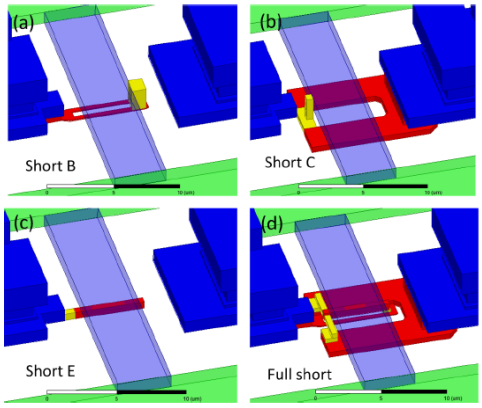

FIGURE 2. Sub-circuits of a single-finger HBT in [6]. Yellow parts are assistance connection structures.

II. 3D EM SIMULATION PARAMETER EXTRACTION METHOD DISCUSSION

Multi-step 3D EM simulation methods like [4] and [5] and our previous works [6], [8] are based on the ideal that simplified inter-device 3D structures are in accordance with specified lumped-element equivalent circuits. Considering the field distribution as a whole system, we find that there are EM field distortion problems in these works which are not noticed yet. The field distortion problem should be avoided to improve the extraction accuracy.

The 3D device model shown in Fig. 1 is a common emitter HBT redraw from [6], and 3D EM simulation sub-circuits are shown in Fig.2. The ''Open'' structure is a reliable simulation structure in EM field analysis for its natural connection with the cut-off device. However, the ''short'' structure sub-circuits would bring serious EM field distortion problems. In ''shortB'' (base shorted) structure, collector and emitter electrodes are omitted, and this structure is designed to extract the base-emitter inductance. This simplified structure is considered as a ''free from others'' sub-circuit [6]. Unfortunately, the inter-electrode impedance depends on the field distribution of the overall device structure at high frequencies, so sub-circuits are not ''free from others''. The key of a precise high-frequency 3D EM parameter extraction is to find some sub-circuits with the field distribution similar with the reference 3D device model (here is the ''open'' structure). Otherwise, EM field distortion will be induced. Comparing the field pattern in Fig.3 (a) (''open'' structure) and (b) (''shortB'' structure), we can find the field pattern distortion is serious. The highest electric field intensity in Fig.3 (a) is 2.4e+7 (V/m), but the electric field intensity in Fig.3 i(b) is 1.6e+6 (V/m). Furthermore, ''Short'' structures have to be applied with assistance structures connecting electrodes. These structures in fact make electrodes had the same electric potential, which is not consistent with HBTs in real working condition. As shown in Fig.3 (c), ''shortC'' (collector shorted) structure, the field pattern is like a plate capacitor between ground plane and collector (red parts indicate the energy concentration area), but the real energy concentration area should be between base and collector when the HBT is under normal biases. This field pattern analysis indicates that the multi-step 3D EM extrinsic parameter extraction method in terahertz band is with pitfalls.

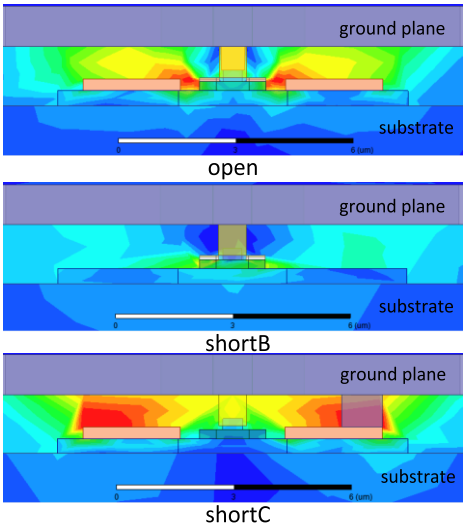

FIGURE 3. Field patterns in sectional view of the "open" structure and other sub-circuits ("shortB" and "shortC") at 220GHz.

Although shortcomings exist, 3D EM simulation parameter extraction approaches still give more precise theoretical inter-electrode parasitics than other methods and promote the development of THz devices, and the inter-electrode impedance plays an important role in THz device modeling. The extrinsic parameter uncertainty induced by improper sub-circuits (some "short" structures mainly) will be bigger in complex structure or multi-finger devices at high frequencies, so a more rigorous parameter extraction approach is needed in 3D EM simulation methods.

III. MODIFIED INTER-ELECTRODE EQUIVALENT-CIRCUIT MODEL AND ASSISTANCE 3D EM SIMULATION STRUCTURES

A. MODIFIED INTER-ELECTRODE EQUIVALENT-CIRCUIT MODEL

In terahertz band, 3D EM inter-electrode impedance extraction methods with too many sub-circuits are improper for complex structure devices. We simplify the inter-electrode impedance equivalent circuit and extract parasitics with only three 3D EM simulation structures-"open", "double-base" and "double-collector". These structures are with less EM field distortion. The modified inter-electrode equivalent-circuit model shows better performance than the old complex one.

The double heterojunction bipolar transistor (DHBT) is produced by Nanjing Electronic Devices Institute (NEDI) with the 0.5-μm InP DHBT technology reported in [15] and [16]. The bottom Metal layer "M1" acts as the "ground" plane in thin-film microstrip line circuits, and it is connected with the emitter contact directly. Pad parasitics are de-embedded by the line-reflect-reflect-match (LRRM) system calibration with open-short de-embedding under 66GHz and thru-reflect-line (TRL) de-embedding over 75GHz in this work. The pad structure is described in [17].

The equivalent-circuit model in Fig.4 is sorted into three parts: the internal device, the inter-electrode impedance, and parasitics of pad and test structure. The inter-electrode impedance equivalent circuit has nine elements. Lbxi, Rbxi, Lcxi, Rcxi, Lexi, and Rexi represent inductors and resistances of electrode contacts and posts. Cbexi, Cbcxi and Ccexi represent inter-electrode capacitances between base-emitter, base-collector and collector-emitter electrodes, respectively. As shown in Fig.5, the internal device topology is the same as the conventional bipolar transistor model in [18]. Within the extraction procedure, Cbcx is very small and omitted.

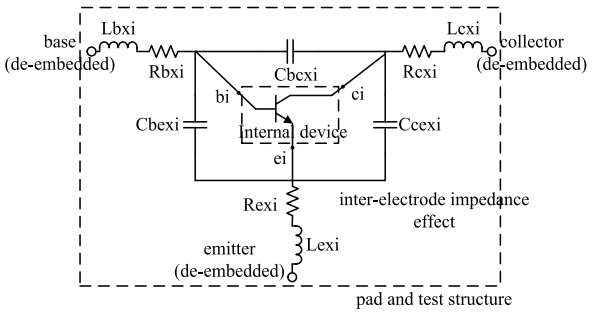

FIGURE 4. Modified InP HBT small-signal equivalent-circuit model. The model is sorted into three parts-the internal device, the inter-electrode impedance and parasitics of pad and test structure.

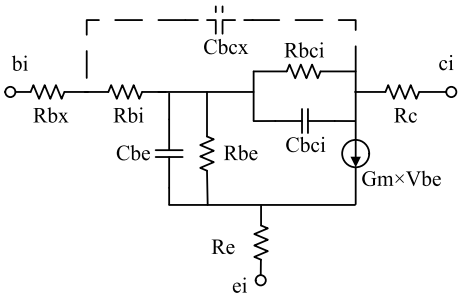

FIGURE 5. Internal device small-signal model.

B. ASSISTANCE 3D EM SIMULATION STRUCTURES

We use only three assistance HFSS models shown in Fig.6 to determine the inter-electrode impedance of the two-finger 0.5um*7um InP DHBT. The device structure is shown in Fig.7. The "open" structure is with base contact and post, collector contact and post, emitter contact and all the epitaxial layers of the transistor. The space between two emitter contacts is 4.5um. In the "double-base" structure, the electrodes on the collector are eliminated, then the electrodes of the base terminal are elongated to connect the base post replicated on the collector end. In the "double-collector" structure, the electrodes on the base are eliminated, then the electrodes of the collector terminal are elongated to connect the collector post replicated on the base end. They are modified "thru" structures.

The "open" structure can reconstruct the field distribution of transistors under cut-off bias. It is also an acceptable

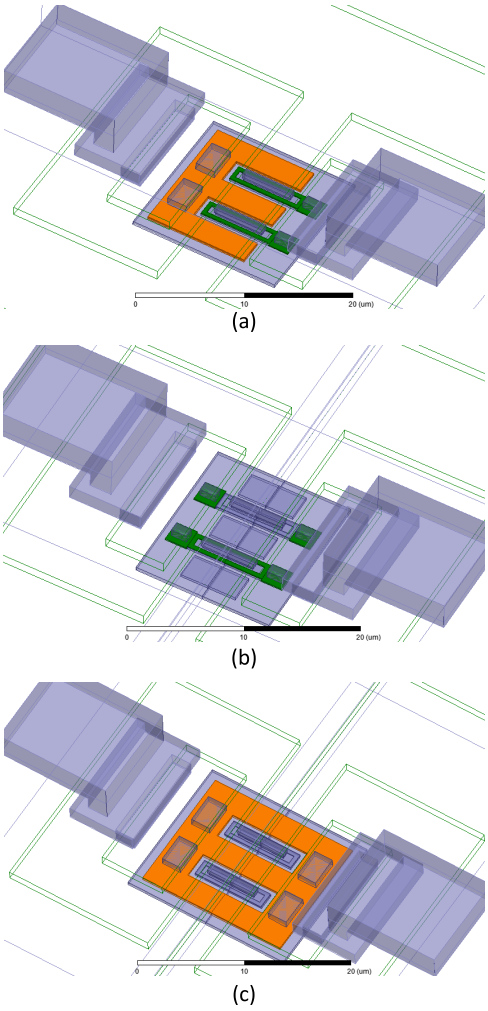

FIGURE 6. 3D models of the two-finger InP DHBT. Emitters are both 0.5um*7um. (a) Open. (b) Double-base. (c) Double-collector.

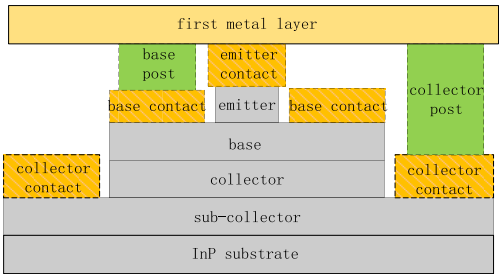

FIGURE 7. Device structure diagram in section view.

simulation structure under normal working biases (base-collector junction reverse biased and base-emitter junction forward biased). In Fig.8, compared with the ''open'' structure, the other two simulation structures, ''double-base'' and ''double-collector'' have the same EM energy concentration region (between base-emitter electrodes). They show much more reliable field distribution than the old assistance 3D model.

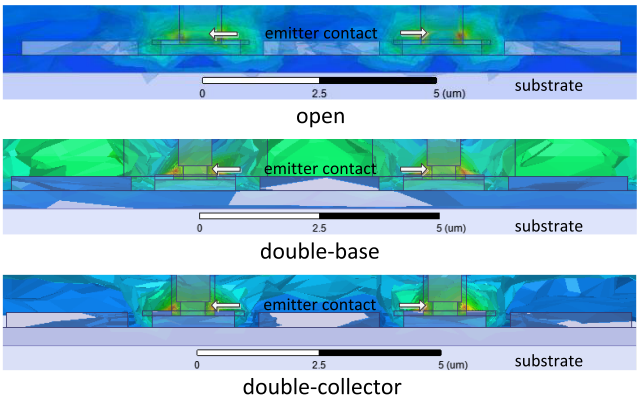

FIGURE 8. EM field distribution (magnitude of E field) at 220 GHz of the three assistance 3D structures in section views. Red parts are energy concentration area. Blue parts are with minimum value.

IV. DISPERSIVE INTER-ELECTRODE IMPEDANCE EXTRACTION AND ANALYSIS

The concept of dispersive impedance in this work is discussed in the introduction. The equivalent circuit is simpler than the past, and the inter-electrode impedance is frequency relevant. Equivalent circuits of the three assistance structures are drawn in Fig.9. The ''open'' structure equivalent circuit is simplified from the equivalent circuit shown in Fig.4. The ''double-base'' structure equivalent circuit is with the repeated base resistance and inductance on the collector end, and a modified inter-electrode capacitance X1*Cbexi is connected with the emitter. In the same way, the ''double-collector'' structure equivalent circuit is with the repeated

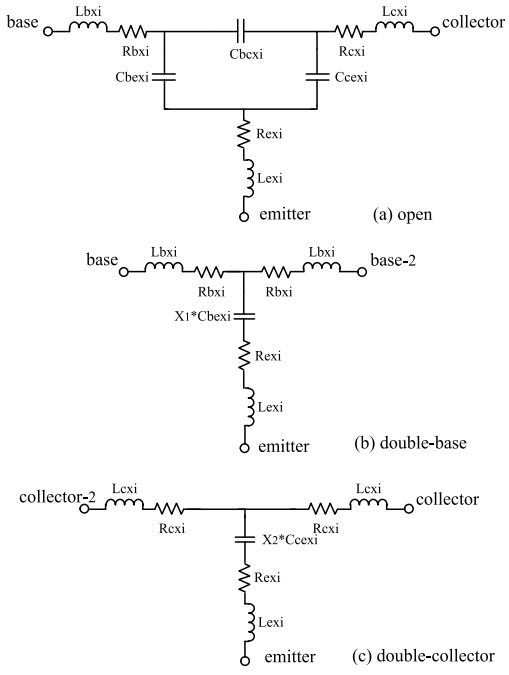

FIGURE 9. Equivalent-circuits of the three 3D EM models, ''open'', ''double-base'' and ''double-collector''.

collector resistance and inductance on the base end, and a modified inter-electrode capacitance X2*Ccexi is connected with the emitter. Parameters X1 and X2 are dispersive capacitance variation factors of assistance sub-circuits. These factors come from structure changes in 3D sub-circuits, which influence the dispersive inter-electrode capacitance. With the precondition that the EM field distribution is not changed much, variation factors can be briefly quantified by the ratio of the maximum EM field intensity of each simulation structure. In the case of the simulated two-finger 0.5um*7um DHBT, X1 is 0.8, and X2 is 0.7.

Z-parameters of the equivalent circuits in Fig.9 can be calculated as follows:

"Open" structure:

$$Z_{11\_open} = j\omega L_{bxi} + R_{bxi} + j\omega L_{exi} + R_{exi} + \frac{1}{j\omega(C_{bexi} + \frac{C_{bcxi}C_{cexi}}{C_{bcxi}+C_{cexi}})} \quad (1)$$

$$Z_{22\_open} = j\omega L_{cxi} + R_{cxi} + j\omega L_{exi} + R_{exi} + \frac{1}{j\omega(C_{cexi} + \frac{C_{bcxi}C_{bexi}}{C_{bcxi}+C_{bexi}})} \quad (2)$$

$$Z_{21\_open} = Z_{12\_open} = j\omega L_{exi} + R_{exi} + \frac{1}{j\omega} \times \frac{1}{C_{cexi} + C_{bexi} + \frac{C_{bexi}C_{cexi}}{C_{bcxi}}} \quad (3)$$

"Double-base" structure:

$$Z_{11\_double\_base} = Z_{22\_double\_base} = j\omega L_{bxi} + R_{bxi} + j\omega L_{exi} + R_{exi} + \frac{1}{X_1 \times j\omega C_{bexi}} \quad (4)$$

$$Z_{21\_double\_base} = Z_{12\_double\_base} = j\omega L_{exi} + R_{exi} + \frac{1}{X_1 \times j\omega C_{bexi}} \quad (5)$$

"Double-collector" structure:

$$Z_{11\_double\_collector} = Z_{22\_double\_collector} = j\omega L_{cxi} + R_{cxi} + j\omega L_{exi} + R_{exi} + \frac{1}{X_2 \times j\omega C_{bexi} + X_3 \times j\omega C_{cexi}} \quad (6)$$

$$Z_{21\_double\_collector} = Z_{12\_double\_collector} = j\omega L_{exi} + R_{exi} + \frac{1}{X_2 \times j\omega C_{bexi} + X_3 \times j\omega C_{cexi}} \quad (7)$$

Then, Rbxi, Lbxi, Rcxi and Lcxi can be directly extracted by:

$$Rbxi = Re(Z_{11\_double\_base} - Z_{21\_double\_base}) \quad (8)$$

$$Lbxi = Im(Z_{11\_double\_base} - Z_{21\_double\_base})/j\omega \quad (9)$$

$$Rcxi = Re(Z_{11\_double\_collector} - Z_{21\_double\_collector}) \quad (10)$$

$$Lcxi = Im(Z_{11\_double\_collector} - Z_{21\_double\_collector})/j\omega \quad (11)$$

After Rbxi, Lbxi, Rcxi and Lcxi are extracted, (1)-(7) can be simplified to:

$$Z_{11\_Op} = LR\_e + \frac{1}{j\omega(C_{bexi} + \frac{C_{bcxi}C_{cexi}}{C_{bcxi}+C_{cexi}})} \quad (12)$$

$$Z_{22\_Op} = LR\_e + \frac{1}{j\omega(C_{cexi} + \frac{C_{bcxi}C_{bexi}}{C_{bcxi}+C_{bexi}})} \quad (13)$$

$$Z_{21\_Op} = LR\_e + \frac{1}{j\omega} \times \frac{1}{C_{cexi} + C_{bexi} + \frac{C_{bexi}C_{cexi}}{C_{bcxi}}} \quad (14)$$

$$Z_{21\_Db} = LR\_e + \frac{1}{X_1 \times j\omega C_{bexi}} \quad (15)$$

$$Z_{21\_Dc} = LR\_e + \frac{1}{X_2 \times j\omega C_{cexi}} \quad (16)$$

Where $Z_{11\_Op} = Z_{11\_open} - j\omega L_{bxi} - R_{bxi}$, $Z_{22\_Op} = Z_{22\_open} - j\omega L_{cxi} - R_{cxi}$, $Z_{21\_Op} = Z_{21\_open}$, $Z_{21\_Db} = Z_{21\_double\_base}$, $Z_{21\_Dc} = Z_{21\_double\_collector}$ and $LR\_e = j\omega L_{exi} + R_{exi}$. There are five complex number equations with five unknowns (Cbexi, Cbcxi, Ccexi, Lexi and Rexi), which can be solved numerically with the already simulated sub-circuits Z-parameters in HFSS. The next step is to find an equation with only one unknown, so we do a formula derivation as follows. Firstly, (15) is transformed to (17), and LR_e is expressed by Cbexi.

$$LR\_e = Z_{21\_Db} - \frac{1}{X_1 \times j\omega C_{bexi}} \quad (17)$$

After (17) is substituted into (16), Ccexi can be expressed by Cbexi:

$$C_{cexi} = \frac{1}{j\omega X_2} \times \frac{1}{Z_{21\_Dc} - Z_{21\_Db} + \frac{1}{X_1 \times j\omega C_{bexi}}} \quad (18)$$

Then, Cbcxi can be expressed by Ccexi and Cbexi with (17) and (18) substituted into (14):

$$C_{bcxi} = \frac{C_{bexi}C_{cexi}}{\frac{1}{j\omega \times (Z_{21\_Op} - Z_{21\_Db} + \frac{1}{j\omega X_1 C_{bexi}})} - C_{cexi} - C_{bexi}} \quad (19)$$

Subsequently, equation (12) can be written as:

$$\frac{1}{\frac{1}{j\omega(Z_{11\_Op} - LR\_e)} - C_{bexi}} = \frac{1}{C_{cexi}} + \frac{1}{C_{bcxi}} \quad (20)$$

After equations (17)-(19) are substituted into (20), the following equation is obtained:

$$\frac{1}{\frac{1}{j\omega(Z_{11\_Op} - Z_{21\_Db} + \frac{1}{j\omega X_1 C_{bexi}})} - C_{bexi}} - \frac{X_2(Z_{21\_Dc} - Z_{21\_Db} + \frac{1}{j\omega X_1 C_{bexi}})}{C_{bexi}(Z_{21\_Op} - Z_{21\_Db} + \frac{1}{j\omega X_1 C_{bexi}})} + \frac{1}{C_{bexi}} = 0 \quad (21)$$

Finally, equation (21) has only one unknown parameter Cbexi. We numerically extract Cbexi at different frequency points to illustrate the dispersive impedance character, which is plotted in Fig.10. LR_e (Rexi and Lexi), Ccexi and Cbcxi are calculated by (17)-(19), respectively. Rbxi, Lbxi, Rcxi and

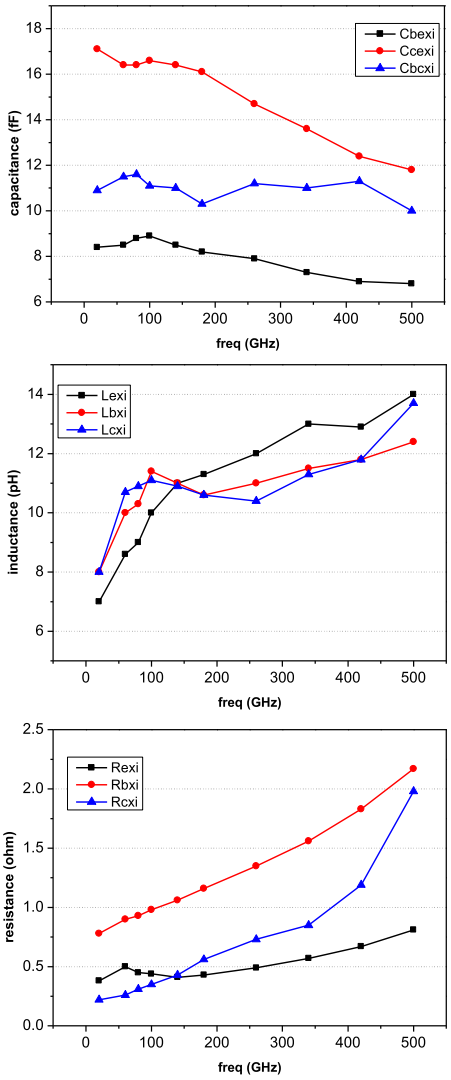

FIGURE 10. Calculated dispersive inter-electrode impedance.

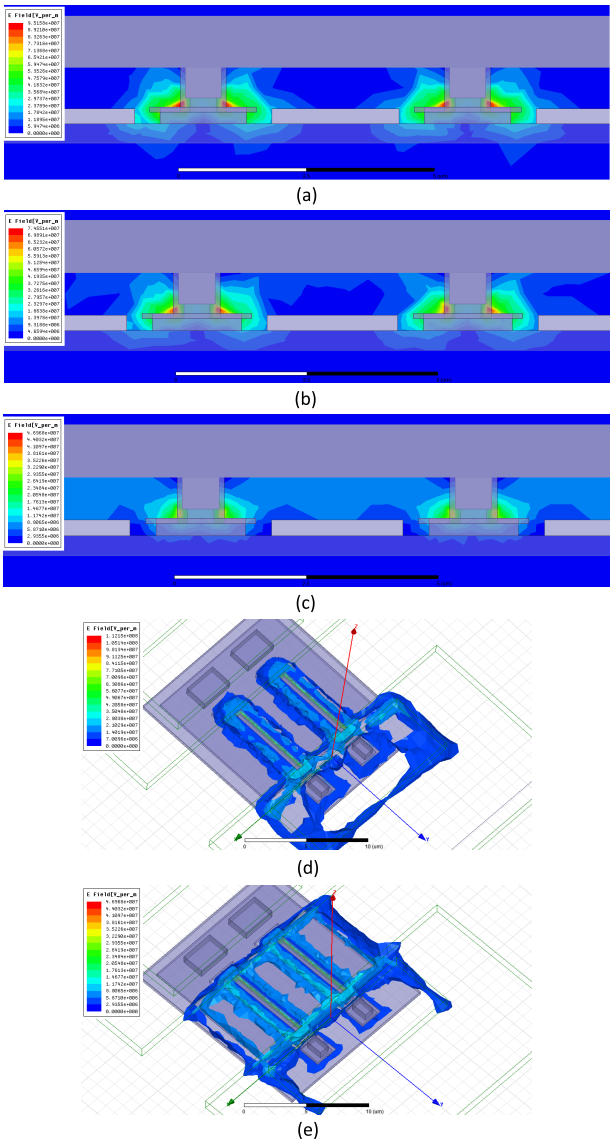

FIGURE 11. Field patterns at different simulation center frequencies. (a)-(c) are sectional views. (d) and (e) are top views.

Lcxi have already extracted by (8)-(11). They are also plotted in Fig.10.

After the 3D EM simulation parameter extraction, it is better to confirm that inter-electrode equivalent circuits are in accordance with the EM field distribution in a broad frequency range. EM field patterns in section view and plan view at different simulation frequencies are shown in Fig.11. The decrease of capacitance, and the increase of resistance and inductance with the rise of frequency can be analyzed from the EM field distribution. With the center frequency going higher, the energy distribution is not concentrated as it was at millimeter-wave frequencies, and therefore we call this phenomenon as EM field discretization. As it is shown in Fig.11(a), the most concentrated EM field energy is between emitter electrode and base electrode (red part). When the frequency exceeds 400GHz, shown in Fig. 11(c), the moderate level EM energy exists extensively (light blue area), and the EM field concentration between emitter electrode and base electrode is not obvious (very little red area, smaller orange and yellow area). At the same time, the EM field energy distributes more between base-collector electrodes, and between the collector electrode and the ''ground'' metal layer. Another phenomenon is the multi-finger device EM field sharing effect. Shown in Fig. 11 (d) and (e), EM field concentration areas in high-frequency devices are not independent, and many metal structures (also some nonmetal structures) in the 3D model impact one equivalent-circuit element in the equivalent-circuit model. For example, as for the collector electrode in the middle of the device, the moderate level EM field (blue area) is coupled tightly with base electrodes on both sides.

V. SMALL-SIGNAL MODEL VERIFICATION

We apply our inter-electrode impedance model on a NEDI two-finger 0.5um*7um InP DHBT with the commercial internal device model [18]. The added inter-electrode impedance

model can improve the model accuracy in THz range, especially for multi-finger devices.

In the first step, pad parasitic elements are de-embedded with LRRM system calibration with open-short de-embedding under 66GHz and TRL de-embedding over 75GHz, as stated in Section II. The dispersive inter-electrode impedance extraction is treated as the second step, and it is demonstrated in Section IV. In the third step, there is an inter-electrode impedance de-embedding procedure [6], which gives a corrected internal network parameter matrix $Y_{internal}$ (it is processed like the open-short correction procedure in [19]).

$$Y_{internal} = (Z_{dut} - Z_{series})^{-1} - Y_{parallel} \tag{22}$$

Where $Y_{internal}$ is the internal device Y-parameter matrix. Z_{dut} is the measured device Z-parameter matrix (after measurement system calibration and pad de-embedding). Z_{series} is the inter-electrode inductance and resistance Z-parameter matrix. $Y_{parallel}$ is the inter-electrode capacitance Y-parameter matrix. In the final step, internal parameters are extracted with the simplified conventional HBT model [18]. In this work, the small-signal measurement is carried out with Agilent 0∼66GHz vector network analyzer 8510C incorporating with separated 75GHz∼110GHz frequency extender and 140GHz∼220GHz frequency extender. Because of the sectionalized measurement system, some measurement discontinuity exists.

The two inter-electrode parameter extraction methods, namely, the one in this paper and the one in [6], are applied simultaneously in the same two-finger InP DHBT for comparison. Both the measured and simulated small-signal results of the device with different 3D EM simulation methods are plotted in Fig.12. As for the extraction method in this work, the inter-electrode inductances are frequency relevant, and average values of inter-electrode capacitances and resistances under 220GHz are used. Inter-electrode impedance and internal device parameter biased under Vc = 1.5V and Ib = 800uA (collector current Ic = 24mA) are listed in TABLE I. The inter-electrode parameters extracted by the method in [6] is Lb = 2.7pH, Lc = 2.8pH, Le = 1.7pH; Rbf = 0.5ohm, Rcf = 0.1ohm, Ref = 0.1ohm; Cpbe = 5.3fF, Cpbc = 7.8fF, Cpce = 9.7fF; Mbe = 0.5pH, Mbc = 0.9pH and Mec = 1.3pH. Compared with the old extraction method, S(1,1), S(1,2) and S(2,2) are improved significantly using the new method, and S(2,1) is also in a good agreement with measured S-parameters. The influence of inter-electrode impedance is in the same order of magnitude to all s-parameters. Well extracted dispersive inter-electrode impedance can significantly reduce the simulation error for S(1,1), S(2,2) and S(1,2). However, the magnitude of S(2,1) is much larger than other S-parameters in high-frequency InP HBTs, and the improvement of S(2,1) is limited. Furthermore, measured and simulated multi-biased S-parameters

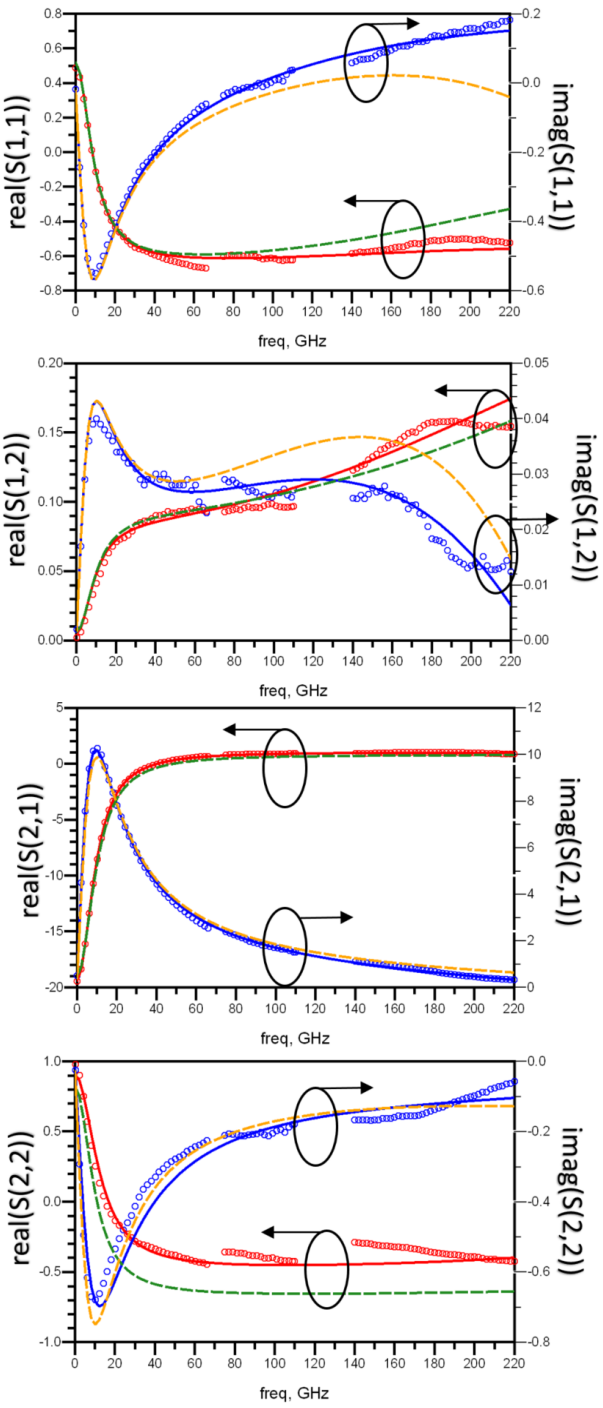

FIGURE 12. Measured and simulated S-parameters of a two-finger 0.5um*7um InP HBT. Measured results are plotted with circles. Simulation results of this work are plotted with solid lines. Simulation results of the previous work are plotted with dash lines.

TABLE 1. Small-signal equavalent circuit elements.

Rbi (Ω)	Re (Ω)	Cbe (fF)	Rbe (Ω)	Cbci (fF)	Rbci (kΩ)	Gm0 (mS)	τ (psec)	Rc (Ω)
32	6.35	190	81	3.2	18.5	534	0.5	1.6
Cbexi (fF)	Ccexi (fF)	Cbcxi (fF)	Lexi (pH)	Lbxi (pH)	Lcxi (pH)	Rexi (Ω)	Rbxi (Ω)	Rcxi (Ω)
8.46	16.24	11.09	6~12	8~11.5	8~11	0.48	1.02	0.41

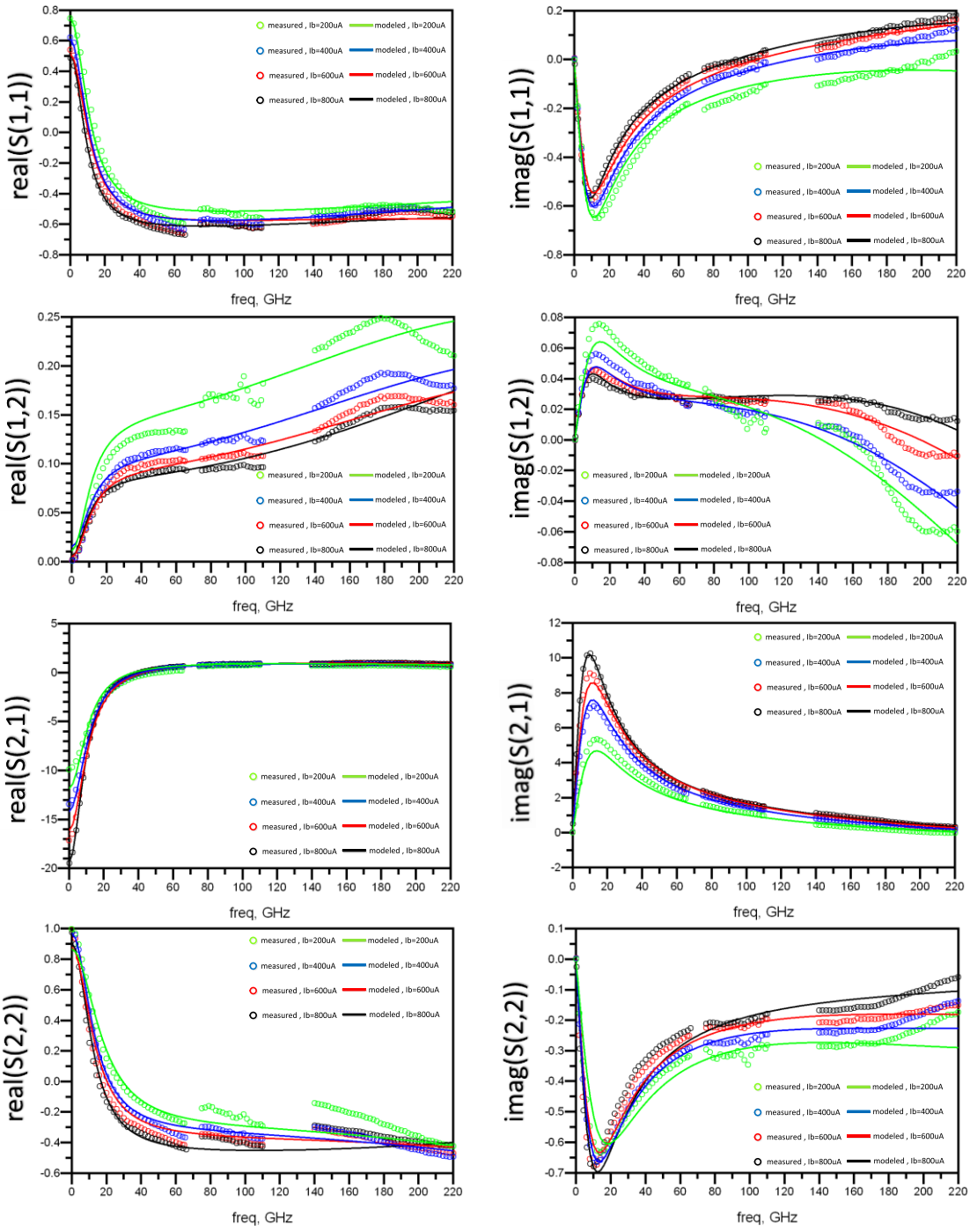

FIGURE 13. Measured and simulated multi-biased S-parameters.

are plotted in Fig.13. Devices are biased under Vc = 1.5V, Ib = 200uA∼800uA stepped by 200uA (collector current Ic = 5.9mA, 13mA, 20.3mA, 24mA, respectively).

VI. CONCLUSION

In this paper, EM field distortion problems in multi-step 3D EM simulation parameter extraction methods are investigated, and the importance of the field distribution conception when modeling high-frequency devices is highlighted. EM field discretization effect and multi-finger device field sharing effect exist in terahertz devices with the rise of the frequency. Therefore, the dispersive inter-electrode impedance model is better for high-frequency device modeling. Comparison between measured and simulated S-parameters demonstrates the feasibility of the proposed 3D EM simulation method in high-frequency multi-finger (or complex structure)

device small-signal modeling. The proposed 3D EM extraction method is much simpler than the old one, and the more rigorous parameter calculation process improves the accuracy of inter-electrode impedance parameters. In the future, special calibration structure devices ''double-base'' and ''double-collector'' will be manufactured. Hardware calibration structure measurement can replace the 3D EM simulation in commercial uses and speed up the parameter extraction process. At the same time, the 3D EM simulation method can be improved with the help of hardware calibration.

REFERENCES

[1] M. Urteaga, Z. Griffith, M. Seo, J. Hacker, and M. J. W. Rodwell, ''InP HBT technologies for THz integrated circuits,'' *Proc. IEEE*, vol. 105, no. 6, pp. 1051–1067, Jun. 2017, doi: 10.1109/JPROC.2017.2692178.

[2] J. C. Rode *et al.*, ''Indium phosphide heterobipolar transistor technology beyond 1-THz bandwidth,'' *IEEE Trans. Electron Devices*, vol. 62, no. 9, pp. 2779–2785, Sep. 2015, doi: 10.1109/TED.2015.2455231.

[3] P. Chevalier *et al.*, ''Si/SiGe: C and InP/GaAsSb heterojunction bipolar transistors for THz applications,'' *Proc. IEEE*, vol. 105, no. 6, pp. 1035–1050, Jun. 2017, doi: 10.1109/JPROC.2017.2669087.

[4] Y. Karisan, C. Caglayan, G. C. Trichopoulos, and K. Sertel, ''Lumped-element equivalent-circuit modeling of millimeter-wave HEMT parasitics through full-wave electromagnetic analysis,'' *IEEE Trans. Microw. Theory Techn.*, vol. 64, no. 5, pp. 1419–1430, May 2016, doi: 10.1109/TMTT.2016.2549520.

[5] Y. Karisan, C. Caglayan, G. C. Trichopoulos, and K. Sertel, ''Distributed modeling of submillimeter-wave HEMT parasitics based on full-wave electromagnetic analysis,'' in *IEEE MTT-S Int. Microw. Symp. Dig.*, Phoenix, AZ, USA, May 2015, pp. 1–3, doi: 10.1109/MWSYM.2015.7167126.

[6] O. Li *et al.*, ''Parasitic parameters extraction for InP DHBT based on EM method and validation up to H-Band,'' *J. Infr., Millim., Terahertz Waves*, vol. 38, no. 5, pp. 583–595, May 2017, doi: 10.1007/s10762-017-0360-7.

[7] Y. Jia, Y. Xu, R. Xu, and Y. Li, ''An accurate parasitic parameters extraction method based on FW-EM for AlGaN/GaN HEMT up to 110 GHz,'' *Int. J. Numer. Model., Electron. Netw., Devices Fields*, vol. 31, no. 1, p. e2270, 2018, doi: 10.1002/jnm.2270.

[8] X. Zhao *et al.*, ''A new inter-electrode coupling capacitance extraction method for deep-submicron AlGaN/GaN HEMTs,'' *IEICE Electron. Express*, vol. 14, no. 15, p. 20170559, Aug. 2017, doi: 10.1587/elex.14.20170559.

[9] T. K. Johansen, V. Krozer, A. Konczykowska, M. Riet, and J. Vidkjr, ''Large-signal modeling of high-speed InP DHBTs using electromagnetic simulation based de-embedding,'' in *IEEE MTT-S Int. Microw. Symp. Dig.*, San Francisco, CA, USA, Jun. 2006, pp. 655–656, doi: 10.1109/MWSYM.2006.249699.

[10] C. M. Snowden, ''Coupled electrothermal and electromagnetic modeling, simulation and design of RF and microwave power FETs,'' in *Proc. Asia–Pacific Microw. Conf.*, Yokohama, Japan, Dec. 2006, pp. 295–304, doi: 10.1109/APMC.2006.4429426.

[11] D. Resca, A. Raffo, A. Santarelli, G. Vannini, and F. Filicori, ''Scalable equivalent circuit FET model for MMIC design identified through FW-EM analyses,'' *IEEE Trans. Microw. Theory Techn.*, vol. 57, no. 2, pp. 245–253, Feb. 2009, doi: 10.1109/TMTT.2008.2011208.

[12] B. Sheinman *et al.*, ''A peeling algorithm for extraction of the HBT small-signal equivalent circuit,'' *IEEE Trans. Microw. Theory Techn.*, vol. 50, no. 12, pp. 2804–2810, Dec. 2002, doi: 10.1109/TMTT.2002.805195.

[13] G. Crupi *et al.*, ''Accurate multibias equivalent-circuit extraction for GaN HEMTs,'' *IEEE Trans. Microw. Theory Techn.*, vol. 54, no. 10, pp. 3616–3622, Oct. 2006, doi: 10.1109/TMTT.2006.882403.

[14] T. K. Johansen, R. Leblanc, J. Poulain, and V. Delmouly, ''Direct extraction of InP/GaAsSb/InP DHBT equivalent-circuit elements from*S*-parameters measured at cut-off and normal bias conditions,'' *IEEE Trans. Microw. Theory Techn.*, vol. 64, no. 1, pp. 115–124, Jan. 2016, doi: 10.1109/TMTT.2015.2503769.

[15] B. Niu *et al.*, ''Fabrication and small signal modeling of 0.5 μm InGaAs/InP DHBT demonstrating F_T/F_{max} of 350/532 GHz,'' *Microw. Opt. Tech. Lett.*, vol. 57, no. 12, pp. 2774–2778, Dec. 2015, doi: 10.1002/mop.29433.

[16] X. Li *et al.*, ''225–255-GHz InP DHBT frequency tripler MMIC using complementary split-ring resonator,'' *J. Infr., Millim., Terahertz Waves*, vol. 38, no. 2, pp. 166–175, Feb. 2017, doi: 10.1007/s10762-016-0325-2.

[17] X. Li *et al.*, ''A thru-halfthru-short de-embedding method for millimeter-wave on-wafer HBT characterization,'' *IEEE Electron Device Lett.*, vol. 38, no. 6, pp. 720–723, Apr. 2017, doi: 10.1109/LED.2017.2693439.

[18] M. Iwamoto *et al.*, ''Large-signal HBT model with improved collector transit time formulation for GaAs and InP technologies,'' in *IEEE MTT-S Int. Microw. Symp. Dig.*, Philadelphia, PA, USA, Jun. 2003, pp. 635–638, doi: 10.1109/MWSYM.2003.1212453.

[19] M. C. A. M. Koolen, J. A. M. Geelen, and M. P. J. G. Versleijen, ''An improved de-embedding technique for on-wafer high-frequency characterization,'' in *Proc. IEEE BCTM*, Sep. 1991, pp. 188–191, doi: 10.1109/BIPOL.1991.160985.

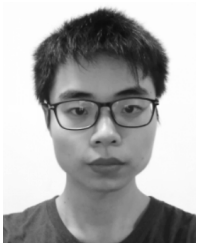

YAPEI CHEN was born in Hebei, China, in 1990. He received the B.S. degree in electromagnetic wave propagation and antenna from the University of Electronic Science and Technology of China, Chengdu, in 2013, where he is currently pursuing the Ph.D. degree in electromagnetic field and microwave techniques.

His current research interests include millimeter-wave and THz monolithic integrated circuit design and modeling of high-frequency InP heterojunction bipolar transistors.

YONG ZHANG (M'05–SM'13) received the B.S., M.S., and Ph.D. degrees from the University of Electronic Science and Technology of China (UESTC), Chengdu, China, in 1999, 2001, and 2004, respectively. He was invited as a Visiting Scholar with the Illinois Institute of Technology, Chicago, IL, USA, from 2009 to 2010. He has been involving in the field of RF circuits for 18 years since he entered the UESTC as a master's student. He is currently a Professor with UESTC because of his outstanding research achievements. He has published more than 100 journals and conference papers. He has applied 13 patents and five of them got the authorization.

His current research interests include the design and application of passive and active components at RF frequencies and solid state terahertz technology.

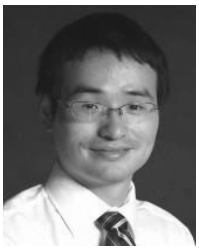

YUEHANG XU (M'11–SM'16) received the B.S. and M.S. degrees in electromagnetic field and microwave techniques from the University of Electronic Science and Technology of China (UESTC), Chengdu, China, in 2004 and 2007, respectively, and the Ph.D. degree from UESTC joint with Columbia University, New York, NY, USA, in 2010.

He joined the Department of Electronic Engineering, UESTC, in 2010 where he has been a Professor since 2017. He was a Visiting Associate Professor with Case Western Reserve University, Cleveland, OH, USA, in 2016. He has authored or co-authored over 150 scientific papers in international journals and conference proceedings. His current research interests include modeling and characterization of radio frequency micro/nano-scale electronic devices and MMIC design.

YAN SUN received the B.S. and M.S. degrees in electromagnetic field and microwave techniques from the University of Electronic Science and Technology of China, Chengdu, China, in 2011 and 2014, respectively.

He joined the Science and Technology on Monolithic Integrated Circuits and Modules Laboratory, Nanjing Electronic Devices Institute, Nanjing, China, in 2014. He is currently involving on the design of InP and GaN millimeter-wave and THz monolithic integrated circuit.

WEI CHENG received the Ph.D. degree from the Institute of Microelectronics, Chinese Academy of Sciences, in 2009. He then joined the Science and Technology on Monolithic Integrated Circuits and Modules Laboratory, Nanjing Electronic Devices Institute, Nanjing, China, in 2009. He is currently involving on the development of InP HBT/DHBT technologies.

HAIYAN LU received the B.S. degree in electronic and information engineering and the M.S. degree in communication and information engineering from the Nanjing University of Science and Technology, Nanjing, China, in 2007 and 2009, respectively.

She joined the Science and Technology on Monolithic Integrated Circuits and Modules Laboratory, Nanjing Electronic Devices Institute, Nanjing, China, in 2009. She is currently involving on the development of THz measurement systems and transistor modeling.

FEI XIAO was born in Sichuan, China, in 1975. He received the B.S. degree in applied physics from the University of Chongqing, Chongqing, China, in 1997, and the M.S. degree in physical electronics and the Ph.D. degree in radio physics from the University of Electronic Science and Technology of China (UESTC), Chengdu, China, in 2002 and 2005, respectively. In 2006, he joined the School of Electronic Engineering, UESTC, as a Teaching Assistant. He has authored or co-authored approximately 20 technical papers. His current research interests are microwave and millimeter-wave devices and computational electromagnetism.

RUIMIN XU (M'07) was born in Sichuan, China, in 1958. He received the B.S. and Ph.D. degrees in electromagnetic field and microwave techniques from the University of Electronic Science and Technology of China (UESTC), Chengdu, China, in 1982 and 2007, respectively.

He is currently a Full Professor with UESTC. His current research interests include microwave and millimeter-wave technologies and applications, and radar systems.